Scale-free correlations, influential neighbours and speed control in flocks of birds

Hemelrijk, Charlotte; Hildenbrandt, Hanno

Published in:
Journal of Statistical Physics

DOI:
10.1007/s10955-014-1154-0

Publication date:
2015

J Stat Phys (2015) 158:563–578
DOI 10.1007/s10955-014-1154-0

Scale-Free Correlations, Influential Neighbours and Speed Control in Flocks of Birds

Charlotte K. Hemelrijk · Hanno Hildenbrandt

Received: 14 March 2014 / Accepted: 17 November 2014 / Published online: 6 December 2014

Abstract Coordination of birds in large flocks is amazing, especially, since individual birds only interact with a few neighbors (the so-called 'influential neighbours'). Yet, empirical data show that fluctuations of velocity and speed of different birds are correlated beyond the influential neighbours and are correlated over a larger distance in a larger flock. This correlation between the correlation length of velocity or speed and flock size was found to be linear, called a scale-free correlation. It depends on the way individuals interact in the flock, for instance, on the number of influential neighbours and speed control. It is unknown however, how exactly the number of influential neighbours affects this scale-free correlation. Recent empirical data show that different degrees of control of speed affect the scale-free correlation for speed fluctuations. Theoretically, based on statistical mechanics, it is predicted that at very high speed control, the correlation is no longer scale-free but saturates at a certain correlation length and this hampers coordination in flocks. We study these issues in a model, called StarDisplay, because its behavioural rules are biologically inspired and many of its flocking patterns resemble empirical data. Our results show that the correlation length of fluctuations of velocity as well as speed correlate with flock size in a scale-free manner. A higher number of influential neighbours causes a diminishing increase of the slope of the scale-free correlation with velocity, resulting thus in flocks that coordinate more uniformly. Similar to recent empirical data higher speed control reduces the correlation length of speed fluctuations in our model. As predicted theoretically, at very high speed control the model generates a non-scale free correlation, and although there are still flocks, they are in the process of disintegrating.

Keywords Flocks of birds · Self-organization · Number of influential neighbours · Spatial dynamics · Scale-free correlation · Speed control · Information transmission

Electronic supplementary material The online version of this article (doi:10.1007/s10955-014-1154-0) contains supplementary material, which is available to authorized users.

C. K. Hemelrijk (✉) · H. Hildenbrandt
Behavioural Ecology and Self-Organisation, Centre for Ecological and Evolutionary Studies, University of Groningen, Nijenborgh 7, 9747AG Groningen, The Netherlands
e-mail: c.k.hemelrijk@rug.nl

1 Introduction

Flocks of birds show remarkable coordination of movement among their members. Examples are the coordinated aerobatics of dunlins (*Calidris alpina*) [1] and the complex aerial maneuvers of huge flocks of starlings (*Sturnus vulgaris*) at dawn above a roosting or sleeping site [2–6]. This complex aerial maneuvering of starlings is amazing, because even though starling flocks may be huge (more than 10.000 individuals), recent studies with the help of stereophotography above Rome [7,8], show that individuals appear to coordinate on average only with a few influential neighbours, the topological range, of about 6 or 7 individuals [9,10]. Yet, individuals appear to be influenced indirectly by others over a longer range, beyond the topological range: in larger flocks the correlation length of the fluctuations of velocity and speed increase with flock size linearly [9]. Larger flocks thus comprise larger units of which the members are observed to coordinate strongly. The size of the units with correlated movement also depends on the number of neighbours with whom individuals interact [18]. The number of influential neighbours may differ between species [10–12]. As to biological advantages, both a high and low numbers of influential neighbours may be adaptive in terms of information transmission and protection against predator attacks [10,13–15].

The size of the clusters of individuals with correlated speed in flocks of starlings (correlation length) have been shown to depend further on the speed control. The correlation length becomes shorter with increasing speed control [16]. Studies in statistical physics predict that at very high speed control the correlation with flock size is no longer scale-free and that this lack of a scale-free correlation should be associated with impaired coordination in flocks of birds [9,16].

To study how the correlation length depends on the number of influential neighbours and speed control, we need a relevant computational model. We choose the computer model, called StarDisplay, because this model concerns flocks whose patterns of flocking emerge automatically from interactions among individuals steered by biologically inspired rules and tuned to biologically relevant parameters and because its patterns of flocking remarkably resemble those of huge flocks of real starlings when flying above the roost in Rome [7,8,17]. Indeed our computational model, StarDisplay, has shown that not only, like in empirical data, in larger flocks the correlation length of the deviation of the velocity from the average is longer and linearly related to flock length, called a scale-free correlation [17], but also that the slope of this correlation is steeper for a greater number of influential neighbours [18]. It has not been studied systematically however how the correlation length and the slope depend on the number of influential neighbours. This is of interest, because correlation length probably affects information transmission. Neither has it been shown how the correlation length of fluctuations of speed depend on flock length and on speed control.

The aim of the present study is to examine these issues systematically in the model, StarDisplay. In it three behavioral rules for coordination of movement based on avoidance, alignment and attraction [19–24] have been combined with the following number of characteristics of birds [8,17]. Modeled individuals fly according to simplified aerodynamics, i.e. they experience lift, drag and the force of gravity [25]. In order to fly along a curve, individuals roll, like real birds do, into the direction of the turn reaching a certain angle to the horizontal plane, the so-called banking angle [26]. The model is parameterized to empirical data of starlings, as regards body weight, speed, lift-drag coefficient [27], roll rate [8], and the way in which the flocks remain above a site for sleeping of size similar to that observed in Rome [2,7]. The resemblance to empirical data of flocking patterns in the model concerns the relative proportions (aspect ratios) of the flocks, their

flat shape, their orientation, and their internal structure as regards the similarity in density between front and back, and the distribution of distances and angles to the nearest neighbours. As to the way flocks turn in the model, the orientation of the flock changes relative to the direction of movement, individuals swap locations, the flock compresses and individuals in the model lose height during turning as in rock doves, starlings, pewits and in steppe eagles [7,28–30]. Resemblance includes further the scale-free correlation between flock size and the correlation length of velocity [17,18], which we study here in more detail.

In the present paper, we show that, while keeping density constant, the correlation length in velocity in flocks in the model increases not only with the flock size [17], but also with the number of influential neighbours (topological range) [18]. We show further that the correlation between the correlation length of fluctuations in speed and flock length is linear and that the correlation length decreases with increasing speed control. At high values for speed control its correlation with flock length saturates and thus becomes non-scale-free. Although the flock still coordinates, it is in the process of collapsing into subgroups in line with theoretical predictions [9,16].

2 Methods

2.1 The Model

2.1.1 General Outline of the Model

Because flying implies movement in all directions, we developed a model in three dimensions. The behaviour of each individual in StarDisplay is based on its cruise speed, its social environment (i.e. the position and heading of its nearby neighbours), its attraction to the roost, the simplified aerodynamics of flight which includes banking while turning, reaction time and random noise, indicating unspecified causes [8,17]. It comprises two causes of error, the random noise and the reaction time, because while waiting to react, the birds still continue to fly (Table 1). Following other studies [19,23,31], we model social coordination in terms of (social) forces. We built the model in SI units and choose real parameter values where available (Table 1). For details of the behavioural rules see Appendix.

2.1.2 Parameterization, Initial Condition and Experiments

We have parameterized individuals in the model to realistic data of birds, especially of starlings, see our earlier version of StarDisplay (Table 1) [8]. Roll rate and banked turns were tuned to those observed in movies of starlings and appear to be within the range measured for other species [32] and to resemble empirical data in that individuals lose height during turns and that they roll into the turn faster than that they roll back [32,33] (Appendix, Eqs. (22) and (23)).

Note that we have kept the distance to the nearest neighbours constant in our simulation-experiments. This is important because otherwise the number of influential neighbours may influence the correlation length ξ via a difference in density.

We study the effect of the number of influential neighbours, i.e. topological range (Table 1). In order to study many flock sizes, we have drawn flock sizes from a geometric distribution of 50.000 individuals. The geometric distribution is given by $P(x = n) = p \cdot (1-p)^{n-1}$ with

Table 1 Parameters of the model

Parameter	Description	Value
N	Flock size (# of individuals)	10–10,000
n_c	Number of interaction partners	2, 3, 4, 6.5, 15, 20, 25
r_{sep}	Separation radius	2.0, 2.3, 2.8, 4.0, 5.5, 7.0, 9.0, 10.0 m
NND_c	Standard nearest neigbour distance	1.2 m
Δt	Integration time step	5 ms
Δu	Reaction time	50 ms
v_0	Cruise speed	10 m/s
m	Mass	0.08 kg
C_L/C_D	Lift-drag coefficient	3.3
L_o	Default lift	0.78 N
D_0, T_0	Default drag, default thrust	0.24 N
$w_{\beta in}$	Banking control	10
$w_{\beta out}$	Banking control	1
w_{sp}	Speed control	1, 0.5 0.1, 0.01, 0.001, 0 1/s
R_{max}	Max. perception radius	100 m
s	Interpolation factor	0.1 Δu
r_h	Radius of max. separation ("hard sphere")	0.2 m
w_s	Weighting factor separation force	1 N
-	Rear "blind angle" cohesion & alignment	2*45°
w_a	Weighting factor alignment force	0.5 N
w_c	Weighting factor cohesion force	1 N
C_c	Critical centrality below which an individual is assumed to be in the interior of a flock.	0.35
w_ξ	Weighting factor random force	0.01 N
R_{Roost}	Boundary radius	150 m
w_{RoostH}	Weighting factor horizontal boundary force	0.01 N/m
w_{RoostV}	Weighting factor vertical boundary force	0.2 N

Top section concerns the parameters in the present study, namely flock size and number of influential neighbours. In order to keep the distance to the nearest neighbours (NND) constant at 1.2 m for higher numbers of influential neighbours, larger radii of separation were used. Bottom section comprises the default parameters of the model [8,17]

$p = 0.1$, obtaining flock sizes ranging between 10 and 10.000 individuals (Table 1). In order to study purely effects of number of flock members and influential neighbours and not of differences in flock density (that usually accompany a higher number of influential neighbours [34]), we increase the separation radius r_{sep} if the number of influential neighbours is higher (Table 1) so that we maintain approximately the same nearest neighbour distance NND_c for the different numbers of influential neighbours.

We investigated values of speed control w_{sp} in Eq. (3) of 0, 1 and 100 (Table 1), by default we used $w_{sp} = 1$ or $w_{sp} = 0$.

At the beginning of each simulation, individuals start with random orientations at random positions inside a cylinder with radius, R_{Roost}. In order to omit effects of initial condition, we have studied patterns after a transitive period of 2 minutes.

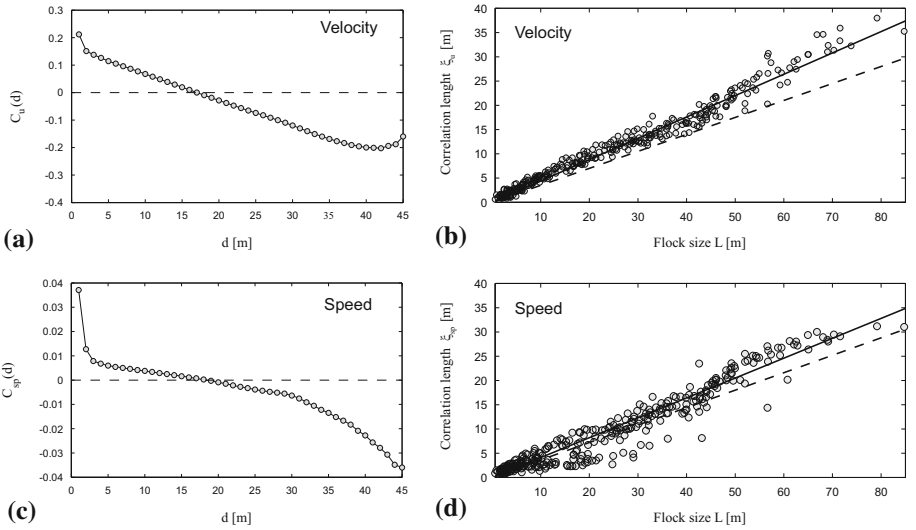

Fig. 1 Correlation length of the deviation from the average of velocity ξ_u and speed ξ_{sp} among individuals in the flocks [17]. **a**, **c** Calculation of a single case of the correlation length is shown for velocity ξ_u (**a**) and speed ξ_{sp} (**c**) for an arbitrary flock size of 1,574 individuals and flock length (largest distance between two flock members) of 45 m and the number of influential neighbours is 6.5. The *dotted line* shows where the correlation function is zero, which indicates the correlation length. **b**, **d** The relation between correlation length and flock size L (in m) is shown for velocity (**b**) and speed (**d**). This includes the case for the flock at the *left*. The slope a_u of the regression line (*solid line*) for velocity in the model is 0.44 (Pearson's correlation test: n = 344, r = 0.98, P $<$ 0.001) and for speed it is a_{sp} = 0.41 (Pearson's correlation test: n = 340, r = 0.96, P $<$ 0.001). Shown as *dashed lines* are the corresponding empirical regression lines from [9] where the slope for velocity a_u is 0.35 and for speed a_{sp} is 0.36

2.2 Measurements

We measured the following properties of a flock: (a) the flock size in terms of its maximum length L, and (b) the correlation length of the fluctuations of the velocity ξ_u and of speed ξ_{sp} among its group members (Fig. 1). Each point in Fig. 1b, d and in the measurement of Fig. 1a, c, corresponds to a time-average of a specific flocking event.

2.2.1 The Maximum Length of the Flock

The maximum length of the flock L is given as the largest distance between two flock members as was done in the empirical study of starling flocks [9].

2.2.2 The Correlation Length of the Fluctuations of the Velocity and Speed

The correlation length of the fluctuations of the velocity among group members ξ_u reflects the size of the domains or sub-flocks of individuals that are temporarily closely correlated in their velocity. We calculate the correlation length ξ_u in three steps as was done for real starlings [9]. First, the deviation $\mathbf{u}_i$ of the velocity of each group member i of that of the average velocity is calculated Eq. (1)

$$\mathbf{u}_i = \mathbf{v}_i - \bar{\mathbf{v}} \qquad \text{Deviation from flock velocity} \quad (1)$$

Here, $\mathbf{v}_i$ is the velocity of individual i, $\bar{\mathbf{v}}$ is the velocity of the centre of gravity. Further, the correlation function of the fluctuations of velocity among all individuals $C_u(d)$ measures the average inner product of the fluctuations of velocity between individuals at distance d Eq. (2):

$$C_u(d) = \frac{1}{c_0} \frac{\sum_{ij} \mathbf{u}_i \mathbf{u}_j \delta(d - d_{ij})}{\sum_{ij} \delta(d - d_{ij})} \quad \text{correlation function} \quad (2)$$

Here, $\delta(d - d_{ij})$ is a smoothed Dirac δ-function, d_{ij} is the distance between two birds and c_0 is a scaling factor such that $C_u(0) = 1$. High values of $C_u(d)$ indicate strong correlations in velocity among all flock members at a certain distance. As is typical in flocks the values of the correlation are greater for short distances and become negative for large distances. The correlation length ξ_u is the distance among birds for which the correlation function is zero (Fig. 1a, c). This value reflects the average size of the correlated domains (i.e. the size of the temporary sub-flocks with strongly coordinated movement). The correlation length of fluctuations in the modulus of velocity, namely speed, ξ_{sp} is calculated similarly replacing velocity by speed. For an example of both, see Fig. 1a, c. Note that in case of high speed control (Fig. 4) where the function $C_{sp}(d)$ drops fast, the function may cross zero at several points. Here, we estimate ξ_{sp} by fitting a line through the points surrounding the average crossing point. We establish ξ_{sp} as the point where this line crosses zero.

3 Results

3.1 Flock Size

An example of the measurement of the correlation length of velocity ξ_u and of speed ξ_{sp} is shown in Fig. 1a, c. For both, velocity and speed, we find that the correlation length is larger in larger flocks. This increase is a positive, linear scale-free correlation between the correlation length of the deviation from the average of the velocity ξ_u and of speed ξ_{sp} with the flock size (Fig. 1b, d). Thus, $\xi_u = a_u L$ and $\xi_{sp} = a_{sp} L$, whereby a represents the slope of the correlation.These scale-free correlations strongly resemble the correlations in empirical data, but their slope a is greater in the model than in empirical data [9]. Thus, temporary sub-flocks are larger.

For studying the effect of the number of influential neighbours, we confine ourselves to the correlation length of velocity ξ_u, because its correlation with flock length L is better understood than that of speed [16].The effects of flock size on the correlation length ξ_u or temporary sub-flocks, can be observed in Fig. 2 and in movies S1–S4 where the deviations of the velocity from the average are colour-coded. Blue indicates no deviation of the average velocity and red indicates the biggest deviation. By comparing for 6 or 7 influential neighbours in the subfigures in Fig. 2a, c and in the movies S1 and S2, the larger flock with the smaller one we see that in the larger flock the size of the temporary sub-flocks (of a single colour), and thus correlation length ξ_u, is larger, the size of the deviations is greater (more red) and that the shape of the flock is more complex.

3.2 Number of Influential Neighbours

For studying the effect of influential neighbours, we increase their number in the model by making individuals interact with 2 up to 25 of their closest neighbours. We do so for flock sizes with the same density drawn from a geometric distribution comprising 10–10.000

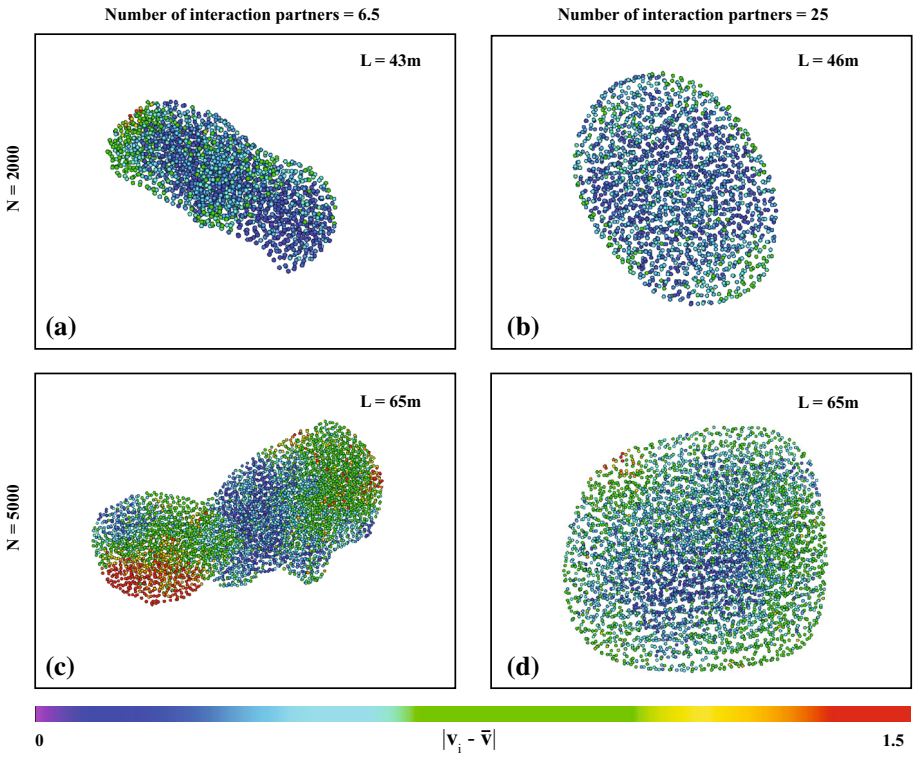

Fig. 2 Snapshots of the deviations of velocity from its average in flocks of different sizes (with 2,000 and 5,000 individuals) and with different number of influential neighbours (topological range 6.5 and 25). For effects of flock size compare snapshots within each *column*, for effects of number of influential neighbours compare snapshots within each *row*. Global velocity deviations from the average range between 0 (*blue*) to 1.5 (*red*), see color scale

individuals. The correlations between correlation length of deviation of velocity ξ_u and flock size L are linear in each case. At larger numbers of influential neighbours, this correlation is steeper (Fig. 3) as is visible from the larger correlation length ξ_u (Fig. 2, movies and compare S1 versus S3 and S2 vs S4). By comparing figures within rows in Fig. 2 and movie S3 versus S1 and movie S4 against S2, we see that the higher number of influential neighbours causes the size of the temporary sub-flocks to be larger and the flock shape to be simpler (being more circular and less convoluted at the border). The slope a_u does neither depend on the number of influential neighbours as a power function (log–log plot in inset of Fig. 3) nor as a logarithmic function (results available in request).

3.3 Speed Control

As to the scale-free correlation between fluctuations of speed and flock size, we investigate whether the correlation length ξ_{sp} reduces at larger values of speed control like in the empirical study (Fig. 4) [16]. In our model a similar parameter of speed control is w_{sp} in Eq. (3). We confirm that indeed, increasing this parameter w_{sp} results in our model in a shorter correlation length ξ_{sp} (inset of Fig. 4) and a lower deviation of speed. In our model we cannot study extreme values for the speed control w_{sp} as studied theoretically by Bialek and co-authors

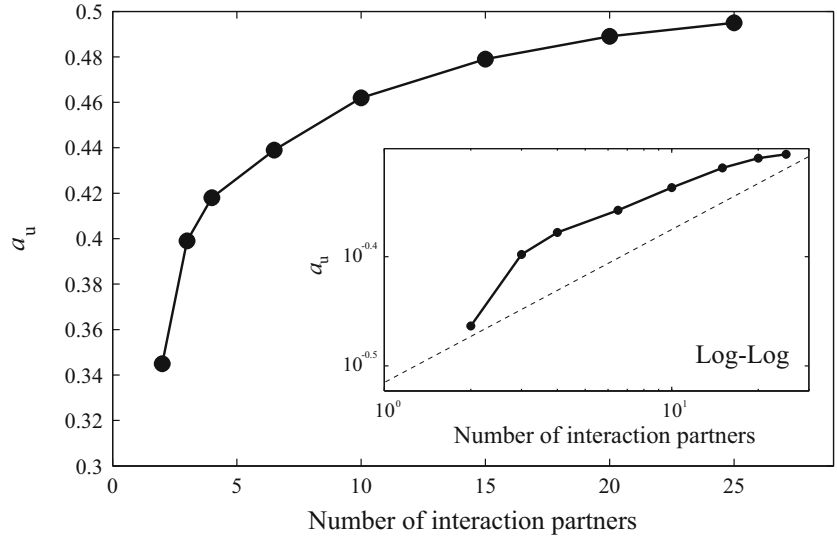

Fig. 3 The effect of the numbers of influential neighbours (topological range) on slope a_u of the linear relationship between the correlation length of velocity ξ_u and the flock size L. *Inset* shows the double-logarithmic plot of the same data. (For calculating the slope we allocated per data-point 50.000 individuals to flocks of different sizes by drawing them from a geometric distribution, see Sect. 2.1.2)

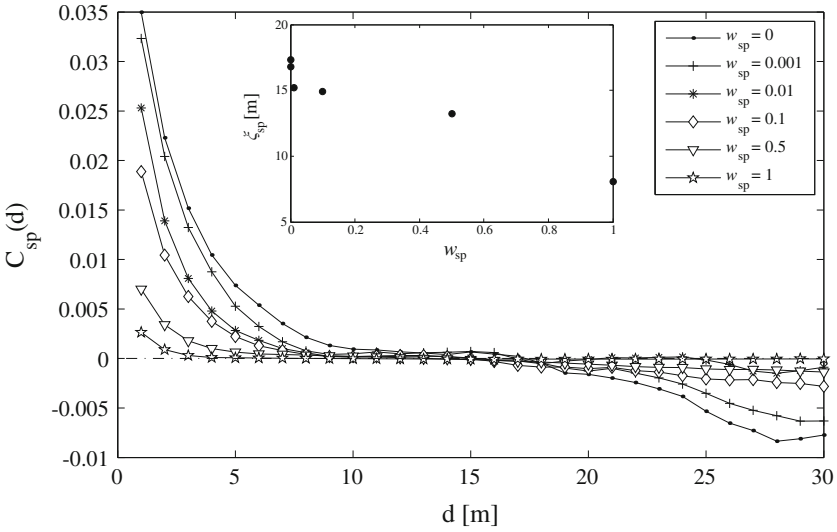

Fig. 4 The correlation function $C_{sp}(d)$ at different values of speed control w_{sp}. *Inset* shows correlation length for speed ξ_{sp} against speed control w_{sp}

[16], for two reasons. First, we cannot decrease the speed control to the very low values, because not only the parameter w_{sp} controls speed in our model (Eq. 3), but also the relative amount of drag and thrust do so (Eqs. 18, 20). Second, we cannot apply extremely strong speed control w_{sp}, because above a certain value of speed control, $w_{sp} > 100$, flocks disintegrate too fast (Fig. 5a). At a reasonably high value of speed control in our model, at w_{sp}=1, the scale

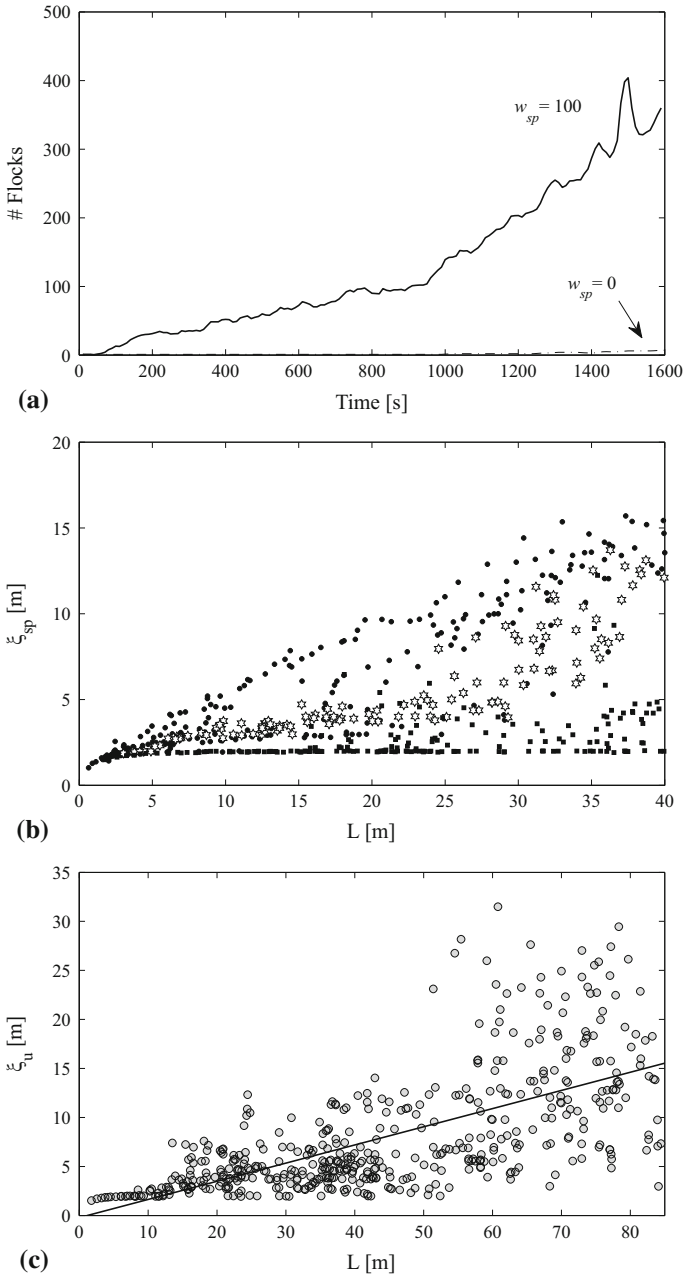

Fig. 5 Effects of high speed control. **a** Splitting of flocks in subflocks (represented by the number of flocks over time, starting with a single flock of 10.000 individuals) at different speed controls of $w_{sp} = 0$ and 100. **b** Correlation between correlation length of the deviation from the average speed ξ_{sp} among individuals and flock length L for different degrees of speed control, $w_{sp} = 0, 1, 100$. At the highest speed control, the correlation is no longer scale-free. Note that $w_{sp} = 0$ (*black dot*), $w_{sp} = 1$ (*open star*) and $w_{sp} = 100$ (*black squares*). **c** At the highest speed control ($w_{sp} = 100$) the relation between correlation length ξ_u and flock size L (in m) is scale free for velocity fluctuations

free correlation between speed fluctuations ξ_{sp} and flock length L is still present (Pearson's correlation $w_{sp} = 1$, n = 155, r = 0.88, P < 0.001) with a reduced slope of $a_u = 0.29$ (Fig. 5b), but at our highest speed control, $w_{sp} = 100$, the correlation between speed fluctuations ξ_{sp} and flock length L is no longer scale free (Fig. 5b). Yet even at this high speed control the correlation with velocity fluctuations is still scale free (Fig 5c, with a reduced slope $a_{sp} = 0.19$, Pearson correlation between flock length L and correlation length of velocity deviations, n = 492, r = 0.659; P < 0.001).

4 Discussion

Our main findings are: First, the correlation lengths of fluctuations of both velocity and speed are associated with flock size in a scale free manner. Second, when the number of influential neighbours is higher, this increases the correlation length and increases the slope of the scale free correlation between the correlation length of velocity fluctuations and flock size. Third, increased speed control reduces the correlation length of speed fluctuations and at its highest value testable in the model ($w_{sp} = 100$), our model shows that the correlation length saturates with increasing flock length. Thus generating a non-scale free correlation. This happens while the flocks are in the process of collapsing.

This scale-free correlation for velocity and speed fluctuations has also been found in an individual-based model with a mixture of topological and metric interaction partners [35].

The greater deviations of velocity from the average of the flock as observed in larger flocks cause the formation of a complex, convoluted border of the flock, because temporarily sub-flocks move in a different direction from their surrounding flock members.

These results resemble those of our models of fish schooling, where schools are simpler in shape if schools are smaller (below 200 individuals) [36].

The slope a of the scale free correlation between correlation length of speed and velocity with flock length strongly resembles those correlations in empirical data, but the slope a is greater in the model than in empirical data [9]. This may be a consequence of the absence of disturbance in the model by, e.g., predators, obstacles and wind [17] and may be due to insufficient speed control.

The steepening of the slope a_u with a higher number of influential neighbours implies that for the same flock size a greater number of influential neighbours causes the flocks to be more synchronised, meaning that temporary sub-flocks are larger and fewer. In other words, flocks move in greater unison when there are more influential neighbours (see movies). This general pattern is in line with our earlier reported instance that in a flock a higher number of influential neighbours resulted in higher synchronisation and therefore in stronger polarisation and in a flock shape that is more static [17]. It is also in line with our findings in models of fish schools [37].

As to the explanation for the longer correlation length with a higher number of influential neighbors, the larger domains of strongly correlated movement are a direct consequence of the adjustment of movement and orientation of individuals to a larger number of neighbors. Because each of the neighbors is also adjusting to more influential neighbors (thus over a longer topological range) the domain of correlated movement (thus the correlation length ξ) obviously increases. Our explanation is mechanistic in terms of the behavior of the individual birds. Here it differs from the explanations inspired by statistical physics [9,16].

We confirm the empirical findings that stronger speed control results in a lower deviation of speed and shorter correlation length [16]. This is understandable in our model because stronger speed control causes the birds to be aligned a much longer period of time and over

a much larger area than lower speed control. At the highest speed control where birds still temporarily flock coherently in our model, but are in the process of slowly disintegrating, the model generates a non-scale free correlation for speed. Yet here the correlation between the correlation length for the fluctuations of velocity ξ_u and flock length L is still scale free. This is in line with the theoretical predictions based on models from statistical physics [9,16].

5 Conclusion

In this paper we study in a computer model, StarDisplay, the internal spatial dynamics in terms of the correlation length of velocity and speed in flocks of birds. The model, StarDisplay, is based on simple behavioural rules (concerned with coordination and with flying) [8,17]. We chose it, because in earlier papers we have shown that flocking patterns emerge in this model that resemble significantly those of real flocks as regards their shape, orientation, turning behaviour and internal dynamics and structure. New results of the present paper are: First, the slope of the scale-free correlation between the correlation length of the fluctuations of velocity and flock length is steeper the higher the number of influential neighbours. Second, in larger flocks the correlation length of the deviation from the average of speed increases linearly, as in flocks of real starlings [9]. Third, when speed is controlled more, the deviation of speed and the correlation length of speed fluctuations decrease like in empirical data; in line with theoretical predictions, at very high speed control, the model generates a non-scale free correlation regarding speed fluctuations and flock length, but still a scale free correlation regarding velocity fluctuations and flock length. Here, the flocks are in the process of collapsing [9,16].

Acknowledgments We are grateful for the grants that have been supporting this research, Hemelrijk's Startup Grant of her Rosalind Franklin Fellowship and her Grant in the European Project of the 7th framework, StarFlag for the work by Hanno Hildenbrandt. We thank the self-organization group for regular discussions.

Appendix: Details of Behavioural Rules

Here, we present the details of the behavioral rules as described in earlier papers [8,17]. Each individual is characterised by its mass, m, its speed, v, and its location, $\mathbf{p}$. Its orientation in space is given by its local coordinate system ($\mathbf{e}_x$, $\mathbf{e}_y$, $\mathbf{e}_z$). Following the model by Reynolds [31], its orientation is indicated by its forward direction, $\mathbf{e}_x$, its sideward direction, $\mathbf{e}_y$, and its upward direction, $\mathbf{e}_z$, which it changes by rotating around these three principal axes (roll, pitch and yaw).

To augment the control over the speed of the individuals that is implicit to the aerodynamic equations (18 and 20), a force, $\mathbf{f}_{\tau_i}$ Eq. (3) is added that brings an individual back to its cruise speed v_0 after it has deviated from it [23].

$$\mathbf{f}_{\tau_i} = m\ w_{sp}(v_0 - v_i) \cdot \mathbf{e}_{x_i} \qquad \text{Speed control} \quad (3)$$

where w_{sp} is a scaling factor, m is the mass of the individual i and v_0 its cruise speed, v_i is its speed, and $\mathbf{e}_{x_i}$ its forward direction.

To make each individual interact with a specific constant number of its closest neighbours (i.e. topological range), each individual i in the model adjusts its metric interaction range, $R_i(t)$ [23] following Eqs. (4) and (5).

$$R_i(t+\Delta u) = (1-s)\, R_i(t) + s\left(R_{\max} - R_{\max}\frac{|N_i(t)|}{n_c}\right) \quad \text{Adaptive interaction range} \tag{4}$$

$$N_i(t) \stackrel{def}{=} \{j \in N\ ;\ d_{ij} \le R_i(t);\ j \neq i\} \quad \text{Neighbourhood of an individual} \tag{5}$$

where Δu is the reaction time, s is an interpolation factor, $R_{\max}$is the maximal metric interaction range, $N_i(t)$ is the neighbourhood of individual i at time t, i.e. the set of neighbours of an individual i which is composed of $|N_i(t)|$ neighbours from the total flock, n_c is the fixed number of topological influential neighbours it strives to have and d_{ij} is the distance between individual i and j given by $\left\|\mathbf{p}_j - \mathbf{p}_i\right\|$ where $\mathbf{p}_i$ gives the position of an individual i. Thus, the radius of interaction at the next step in reaction-time, $R_i(t+\Delta u)$, increases whenever the number of influential neighbours $|N_i(t)|$ is smaller than the targeted number n_c, and it is decreased if it is larger than that; it remains as before if $|N_i(t)|$ equals n_c. Here R_i can neither decrease below the hard sphere in which individuals are maximally avoiding each other r_h Eq. (6) nor increase beyond $R_{\max}$. s, the interpolation factor, determines the step-size of the changes and thus, the variance of the number of actual influential neighbours.

As to separation, individual i is led by a force $\mathbf{f_{s_i}}$to move in the opposite direction of the average direction of the locations of the $|N_i(t)|$ others in its neighbourhood. Following others [19,38], we have omitted the blind angle at the back Eq. (6). We gave individuals a hard sphere with radius r_h as mentioned above, in which they avoid each other maximally Eq. (6). Outside the hard sphere, but inside the radius of separation r_{sep}, the degree of avoidance of others decreases with the distance to the neighbour following a halved Gaussian, $g(x)$, with σ the standard deviation of the Gaussian set so that at the border of the separation zone the force is almost zero, $g(r_{sep}) = 0.01$ Eq. (6).

$$\mathbf{f}_{s_i} = -\frac{w_s}{|N_i(t)|}\sum_{i\in N_i(t)} g(d_{ij})\,\mathbf{d}_{ij};\ \begin{cases} g(d_{ij}) = 1 & ;\ d_{ij} \le r_h \\ \exp\left(-\frac{(d_{ij}-r_h)^2}{\sigma^2}\right) & ;\ d_{ij} > r_h \end{cases} \quad \text{Separation} \tag{6}$$

Here, $|N_i(t)|$ is the number of individuals in the neighbourhood of interaction Eq. (5) and d_{ij} is the distance from individual i to individual j. The direction from individual i to individual j is specified by the unit vector $\mathbf{d}_{ij} = (\mathbf{p}_j - \mathbf{p}_i)/\left\|\mathbf{p}_j - \mathbf{p}_i\right\|$ and w_s is the weighting factor for separation (Tab. 1).

As to cohesion, individual i is attracted by a force $\mathbf{f_{c_i}}$ to the direction of the centre of mass (i.e. the average x, y, z position) of the group of $\left|N_i^*(t)\right|$ individuals located in its topological neighbourhood, but not in its blind angle, in a way similar to models of others [19,20,22,24,39]. Here, w_c is the weighing factor for cohesion Eq. (7) (Table 1). Within the radius of the hard spherer_h, we ignore cohesion with others Eq. (7). To represent fear of predators [40] and build a sharp boundary of the flock [7], we make individuals cohere more strongly when they are at the border of the flock than in its interior by multiplying the force of cohesion by a factor indicating the degree to which an individual is peripheral Eqs. (7) and (9). This factor, called 'centrality' in the group, $C_i(t)$, we calculate as the length of the average vector of the direction of all its neighbours β_{in} relative to the individual i [41]. A high value indicates that the individual is peripheral; a lower value indicates that it is located more in the centre of the group. The 'neighbouring' individuals are all $|N_G(t)|$ individuals in a radius of twice the actual perceptual distance of the individual i Eq. (9).

$$\mathbf{f}_{c_i} = C_i(t)\frac{w_c}{|N_i^*(t)|}\sum_{j\in N_i^*} \mathrm{X}_{ij}\,\mathbf{d_{ij}};\ X_{ij} = \begin{cases} 0\ ;\ d_{ij} \le r_h \\ 1\ ;\ d_{ij} > r_h \end{cases} \quad \text{Cohesion} \tag{7}$$

$$N_i^*(t) = \{\ j \in N_i(t)\ ;\ j \text{ not in the 'blind angle' of } i\ \} \quad \text{Reduced neighbourhood} \quad (8)$$

$$C_i(t) = \frac{1}{|N_G(t)|} \left\| \sum_{j \in N_G(t)} \mathbf{d_{ij}} \right\| ;\ N_G(t) = \{j \in N\ ;\ d_{ij} \leq 2R_i(t);\ j \neq i\} \quad (9)$$

As regards its alignment behaviour Eq. (10), individual i feels a force, $\mathbf{f}_{a_\mathbf{i}}$, to align with the average forward direction of its $\left|N_i^*(t)\right|$ interaction neighbours (the same neighbours as to whom it is attracted).

$$\mathbf{f_{a_i}} = w_a \left(\sum_{j \in N_i^*(t)} \mathbf{e_{x_j}} - \mathbf{e_{x_i}} \right) \Big/ \left\| \sum_{j \in N_i^*(t)} \mathbf{e_{x_j}} - \mathbf{e_{x_i}} \right\| \quad \text{Alignment} \quad (10)$$

Here, $\mathbf{e_{x_i}}$ and $\mathbf{e}_{x_j}$ are the vectors indicating the forward direction of individuals direction of individuals i and j and w_a is the fixed weighting factor for alignment (Table 1).

The 'social force' is the sum of these three forces Eq. (11).

$$\mathbf{F}_{Social_i} = \mathbf{f_{s_i}} + \mathbf{f}_{a_i} + \mathbf{f_{c_i}} \quad \text{Social force} \quad (11)$$

Individuals fly at a similar height above the sleeping site like real starlings [2], because we made them experience both in a horizontal and vertical direction a force of attraction $\mathbf{f}_{Roost}$ to the 'roosting area' Eqs. (12, 13, 14). The strength of the horizontal attraction, $\mathbf{f}_{RoostH}$, is greater, the more radially it moves away from the roost; it is weaker if it is already returning. The strength is calculated using the dot product, i.e. the angle between the forward direction of individual i, $\mathbf{e_{x_i}}$, and the horizontal outward-pointing normal $\mathbf{n}$ of the boundary. The range of the result $[-1..1]$ is transformed to $[0..1]$ by halving the dot product and summing it with a 1/2. The actual direction of the horizontal attraction force to the roost is given by $\mathbf{e}_{y_\mathbf{i}}$ which is the individual's lateral direction. The sign in Eq. (13) is chosen to reduce the outward heading. The actual direction of the horizontal attraction force is given by $\mathbf{e}_{y_\mathbf{i}}$ which is the individual's lateral direction. Vertical attraction, $\mathbf{f}_{RoostV}$, is proportional to the vertical distance from the preferred height z_0 above the roost (arbitrarily called the zero level). Here $\mathbf{z}$ is the vertical unit vector. w_{RoostH} and w_{RoostV} are fixed weighting factors.

$$\mathbf{f}_{Roost_i} = \mathbf{f}_{RoostH_i} + \mathbf{f}_{RoostV_i} \quad \text{Roost attraction} \quad (12)$$

$$\mathbf{f}_{RoostH_i} = \pm w_{RoostH} \left(\frac{1}{2} + \frac{1}{2} \left(\mathbf{e}_{x_i} \cdot \mathbf{n} \right) \right) \cdot e_{y_i} \quad \text{Horizontal} \quad (13)$$

$$\mathbf{f}_{RoostV_i} = -w_{RoostV} \left(p_{x_i} - z_0 \right) \cdot z; \quad z = (0, 0, 1)^T \quad \text{Vertical} \quad (14)$$

The random force indicates unspecified stochastic influences Eq. (15) with ζ being a random unit vector from a uniform distribution and w_ζ being a fixed scaling factor. The sum of the social force, the forces that control speed and ranging and the random force is labeled as 'steering force' Eq. (16).

$$\mathbf{f_{\xi_i}} = w_\xi \cdot \boldsymbol{\xi} \quad \text{Random force} \quad (15)$$

$$\mathbf{F}_{Steering_i} = \mathbf{F}_{Social_i} + \mathbf{f}_{\tau_i} + \mathbf{f}_{Roost_i} + \mathbf{f}_{\zeta_i} \quad \text{Steering force} \quad (16)$$

Physics of flight in the model follows the standard equations of fixed wing aerodynamics which link the lift L, the drag D and the thrust T produced by a bird to attain its current speed v Eq. (17):

$$L = \frac{1}{2}\rho S v^2 C_L \qquad D = \frac{1}{2}\rho S v^2 C_D \qquad \text{Lift and drag} \quad (17)$$

$$L_0 = \frac{1}{2}\rho S v_0^2 C_L = mg;\ D_0 = \frac{1}{2}\rho S v_0^2 C_D = T_0 \qquad \text{Lift and drag at cruise speed } v_0 \quad (18)$$

$$L_i = \frac{v_i^2}{v_0^2} L_0 = \frac{v_i^2}{v_0^2} mg;\ D_i = \frac{C_D}{C_L} L_i = \frac{C_D}{C_L}\frac{v_i^2}{v_0^2} mg \qquad \text{Simplified lift and drag} \quad (19)$$

where ρ is the density of the air and S represents the wing area of the bird (of identical size for all birds). The quotient of C_L and C_D of the dimensionless lift and drag coefficients in the model is fixed, resembling the almost fixed ratio in reality [25]. When a bird is flying horizontally while maintaining a constant cruise speed v_0 its lift balances its weight mg (mass times gravity) and its thrust balances its drag Eq. (18). Division of L by L_0 and of D by L in Eqs. (17) and (18) yields Eq. (19) in which the lift and the drag only depend on the actual speed.

Gravity is directed towards the global 'down' direction, $\mathbf{g} = (0, 0, -g)$, the lift upwards operates towards the local 'up' direction $\mathbf{e}_z$ of the bird and the drag is pointing in the direction opposite to its actual 'forward' direction $\mathbf{e}_x$. Thus, the flight forces are:

$$\mathbf{F}_{Flight_i} = (\mathbf{L}_i + \mathbf{D}_i + \mathbf{T}_0 + m\mathbf{g});\ \mathbf{L}_i = \mathbf{L}_i \cdot \mathbf{e}_{z_i};\ \mathbf{D}_i = -D_i \cdot \mathbf{e}_{x_i};\ \mathbf{T}_0 = T_0 \cdot \mathbf{e}_{x_i} \quad \text{Flight forces} \quad (20)$$

Note that the force $\mathbf{D_i} + \mathbf{T}_0$ counteracts deviations from cruise speed. This speed control remains if we set w_{sp} to zero (3).

Real birds roll into the turn in order to make turns [26]. Because in the absence of external influence we assume that birds 'intend' to fly with their wings at a horizontal level in order to move straightforward, we give the model-birds a tendency to roll back. To represent banked turns, we first calculate the degree to which individuals want to turn, i.e. their lateral acceleration, $\mathbf{a}_l$, which is exerted by the steering force. Banking implies that the individual rolls around its forward axis in the direction of its lateral acceleration, $\mathbf{a}_l$. The lateral acceleration follows the first law of Newton ($\mathbf{F} = m \cdot \mathbf{a}$),

$$\mathbf{a}_{l_i} = \left(\frac{\mathbf{F}_{Steering_i} \cdot \mathbf{e}_{y_i}}{m}\right) \cdot \mathbf{e}_{y_i} \qquad \text{Lateral acceleration} \quad (21)$$

$$\tan(\beta_{in_i}) = w_{\beta_{in}} \left\| \mathbf{a}_{l_i} \right\| \Delta t \qquad \text{Roll in} \quad (22)$$

$$\tan(\beta_{out_i}) = w_{\beta_{out}} \sin(\beta_i) \Delta t \qquad \text{Roll out} \quad (23)$$

$$\beta_i(t + \Delta t) = \beta_i(t) + \beta_{in_i} - \beta_{out_i} \qquad \text{Banking angle} \quad (24)$$

where β_i is the actual banking angle, $w_{\beta_{in}}$ and $w_{\beta_{out}}$, respectively are the weights for rolling in and out the curve of turning, Δt is the update time and β_{in} and β_{out} are the angles over which an individual intends to move inwards and outwards. The tendency to roll into the turn increases with the strength of the tendency to turn sideways, which is due to the urge to coordinate with its topological neighbours (via attraction, alignment and avoidance) and to stay above the roost Eq. (22). Once an individual has banked in the model, its tendency to roll back to the horizontal is proportional to its actual banking angle Eq. (23). The actual banking angle Eq. (24) is the sum of the current angle and the tendencies to roll-in and to roll-out. The ratio of $w_{\beta_{in}}$ and $w_{\beta_{out}}$ determines the roll rate. Note that by banking the individual creates a centripetal force at the cost of lift. Consequently it temporarily tends to move downwards.

After summing the forces of steering and flying, we use Euler integration to calculate the position and velocity at the end of each time-step Δt:

$$\mathbf{v}_i(t+\Delta t) = \mathbf{v}_i(t) + \frac{1}{m}\left(F_{Steering_i}(t) + F_{Flight_i}(t)\right)\Delta t \tag{25}$$

$$\mathbf{p}_i(t+\Delta t) = \mathbf{p}_i(t) + \mathbf{v}_i(t+\Delta t)\cdot\Delta t \tag{26}$$

where $\mathbf{v}_i$ is the velocity of individual i, m its mass, $\mathbf{p}_i$ its location, and Δt is the update time. For the default values, see Table 1.

References

1. Davis, M.J.: The coordinated aerobatics of dunlin flocks. Anim. Behav. **28**(3), 668–673 (1980)
2. Carere, C., Montanino, S., Moreschini, F., et al.: Aerial flocking patterns of wintering starlings, Sturnus vulgaris, under different predation risk. Anim. Behav. **77**, 101–107 (2009)
3. Clergeau, P.: Flocking behavior of starlings (*sturnus vulgaris*) during the day: a gradual gathering to the roost. J. Ornithol. **131**(4), 458–460 (1990)
4. Feare, C.J.: The Starling. Oxford University Press, Oxford (1984)
5. Brodie, J.: The flight behaviour of starlings at a winter roost. Br. Birds **69**, 51–60 (1976)
6. Eastwood, E., Isted, G.A., Rider, G.C.: Radar ring angles and the roosting behaviour of starlings. Proc. R. Soc. Lond. B **156**(963), 242–267 (1962)
7. Ballerini, M., Cabibbo, N., Candelier, R., et al.: Empirical investigation of starling flocks: a benchmark study in collective animal behaviour. Anim. Behav. **76**(1), 201–215 (2008)
8. Hildenbrandt, H., Carere, C., Hemelrijk, C.K.: Self-organized aerial displays of thousands of starlings: a model. Behav. Ecol. **21**(6), 1349–1359 (2010). doi:10.1093/beheco/arq149
9. Cavagna, A., Cimarelli, A., Giardina, I., et al.: Scale-free correlations in starling flocks. PNAS **107**(26), 11865–11870 (2010)
10. Ballerini, M., Cabibbo, N., Candelier, R., et al.: Interaction ruling animal collective behaviour depends on topological rather than metric distance: evidence from a field study. PNAS **105**(4), 1232–1237 (2008)
11. Lukeman, R., Li, Y., Edelstein-Keshet, L.: Inferring individual rules from collective behavior. PNAS **107**(28), 12576–12580 (2010)
12. Nagy, M., Ákos, Z., Biro, D., Vicsek, T.: Hierarchical group dynamics in pigeon flocks. Nature **464**(7290), 890–893 (2010)
13. Inada, Y., Kawachi, K.: Order and flexibility in the motion of fish schools. J. Theor. Biol. **214**(3), 371–387 (2002)
14. Mirabet, V., Pierre, F., Christophe, L.: Factors affecting information transfer from knowledgeable to naive individuals in groups. Behav. Ecol. Sociobiol. **63**(2), 159–171 (2008)
15. Lemasson, B.H., Anderson, J.J., Goodwin, R.A.: Collective motion in animal groups from a neurobiological perspective: the adaptive benefits of dynamic sensory loads and selective attention. J. Theor. Biol. **261**(4), 501–510 (2009)
16. Bialek, W., Cavagna, A., Giardina, I., et al.: Social interactions dominate speed control in poising natural flocks near criticality. Proc. Natl. Acad. Sci. USA **111**(20), 7212–7217 (2014)
17. Hemelrijk, C.K., Hildenbrandt, H.: Some causes of the variable shape of flocks of birds. PLoS One **6**(8), e22479 (2011)
18. Hemelrijk, C.K., Hildenbrandt, H.: Schools of fish and flocks of birds: their shape and internal structure by self-organization. Interface Focus **2**(6), 726–737 (2012)
19. Couzin, I.D., Krause, J., James, R., Ruxton, G.D., Franks, N.R.: Collective memory and spatial sorting in animal groups. J. Theor. Biol. **218**(1), 1–11 (2002)
20. Huth, A., Wissel, C.: The simulation of the movement of fish schools. J. Theor. Biol. **156**(3), 365–385 (1992)
21. Huth, A., Wissel, C.: The simulation of fish schools in comparison with experimental data. Ecol. Model. **75**(76), 135–145 (1994)
22. Kunz, H., Hemelrijk, C.K.: Artificial fish schools: collective effects of school size, body size, and body form. Artif. Life **9**(3), 237–253 (2003)
23. Hemelrijk, C.K., Hildenbrandt, H.: Self-organized shape and frontal density of fish schools. Ethology **114**, 245–254 (2008)
24. Reuter, H., Breckling, B.: Selforganization of fish schools: an object-oriented model. Ecol. Model. **75**, 147–159 (1994)

25. Norberg, U.M.: Vertebrate Flight: Mechanics, Physiology, Morphology, Ecology and Evolution, vol. 27. Springer, New York (1990)
26. Videler, J.J.: Avian Flight. Oxford University Press, Oxford (2005)
27. Ward, S., Mueller, U., Rayner, J.M.V., Jackson, D.M., Nachtigall, W., Speakman, J.R.: Metabolic power of european starlings sturnus vulgaris during flight in a wind tunnel, estimated from heat transfer modelling, doubly labelled water and mask respirometry. J. Exp. Biol. **207**(Pt 24), 4291–4298 (2004)
28. Pomeroy, H., Heppner, F.: Structure of turning in airborne rock dove (Columba livia) flocks. Auk **109**(2), 256–267 (1992)
29. Gillies, J.A., Thomas, A.L.R., Taylor, G.K.: Soaring and manoeuvring flight of a steppe eagle aquila nipalensis. J. Avian Biol. **42**(5), 377–386 (2011)
30. Selous, E.: Thought Transference (or what?) in Birds. Constanble and Company Ltd., London (1931)
31. Reynolds, C.W.: Flocks, herds and schools: a distributed behavioral model. In: Proceedings of the 14th annual conference on computer graphics and interactive techniques. Vol 21. ACM, New York, pp. 25–34 (1987)
32. Gillies, J.A., Bacic, M., Yuan, F.G., Thomas, A.L.R., Taylor, G.K.: Modeling and identification of steppe eagle (aquila nipalensis) dynamics. AIAA Modeling and Simulations Technologies Conference and Exhibit. American Institute of Aeronautics and Astronautics, Honolulu, Hawaii, pp. 18–21 (2008)
33. Taylor, G.K., Bacic, M., Carruthers, A.C., Gillies, J., Ozawa, Y., Thomas, A.L.R.: Flight control mechanisms in birds of prey. 45th AIAA Aerospace Sciences Meeting and Exhibit. American Institute of Aeronautics and Astronautics, Reno, Nevada, pp. 8–11 (2007)
34. Viscido, S.V., Parrish, J.K., Grunbaum, D.: The effect of population size and number of influential neighbors on the emergent properties of fish schools. Ecol. Model. **183**(2–3), 347–363 (2005)
35. Niizato, T., Gunji, Y.: Fluctuation-driven flocking movement in three dimensions and scale-free correlation. PloS One **7**(5), e35615 (2012)
36. Kunz, H., Hemelrijk, C.K.: Simulations of the social organization of large schools of fish whose perception is obstructed. Appl. Anim. Behav. Sci. **138**(3–4), 142–151 (2012)
37. Kunz, H., Hemelrijk, C.K.: Simulations of the social organization of large schools of fish whose perception is obstructed. Appl. Anim. Behav. Sci. **138**(3–4), 142–151 (2012)
38. Zheng, M., Kashimori, Y., Hoshino, O., Fujita, K., Kambara, T.: Behavior pattern (innate action) of individuals in fish schools generating efficient collective evasion from predation. J. Theor. Biol. **235**(2), 153–167 (2005)
39. Hemelrijk, C.K., Kunz, H.: Density distribution and size sorting in fish schools: an individual-based model. Behav. Ecol. **16**(1), 178–187 (2005)
40. Hamilton, W.D.: Geometry for the selfish herd. J. Theor. Biol. **31**, 295–311 (1971)
41. Hemelrijk, C.K., Wantia, J.: Individual variation by self-organisation: a model. Neurosci. Biobehav. Rev. **29**(1), 125–136 (2005)